Annals of Botany **129**: 403–413, 2022
https://doi.org/10.1093/aob/mcab152, available online at www.academic.oup.com/aob

ANNALS OF BOTANY
Founded 1887

MYB42 inhibits hypocotyl cell elongation by coordinating brassinosteroid homeostasis and signalling in *Arabidopsis thaliana*

Yamei Zhuang,[1,2] Wenjun Lian,[1] Xianfeng Tang,[2,*] Guang Qi,[3] Dian Wang,[4] Guohua Chai,[1,*] and Gongke Zhou[1,*]

[1]College of Resources and Environment, Qingdao Agricultural University, Qingdao 266109, China, [2]Qingdao Institute of BioEnergy and Bioprocess Technology, Chinese Academy of Sciences, Qingdao 266101, China, [3]State Key Laboratory of Wheat and Maize Crop Science and College of Agronomy, Henan Agricultural University, Zhengzhou 450002, China, and [4]College of Agronomy, Qingdao Agricultural University, Qingdao 266109, China
** For correspondence. E-mail chaigh@qau.edu.cn or zhougk@qau.edu.cn*

Received: 3 December 2021 Returned for revision: 11 October 2021 Editorial decision: 14 December 2021 Accepted: 15 December 2021
Electronically published: 18 December 2021

• **Background and Aims** The precise control of brassinosteroid (BR) homeostasis and signalling is a prerequisite for hypocotyl cell elongation in plants. Arabidopsis MYB42 and its paralogue MYB85 were previously identified to be positive regulators of secondary cell wall formation during mature stages. Here, we aim to reveal the role of MYB42 and MYB85 in hypocotyl elongation during the seedling stage and clarify how MYB42 coordinates BR homeostasis and signalling to regulate this process.
• **Methods** Histochemical analysis of *proMYB42-GUS* transgenic plants was used for determination of the *MYB42* expression pattern. The *MYB42*, *85* overexpression, double mutant and some crossing lines were generated for phenotypic observation and transcriptome analysis. Transcription activation assays, quantitative PCR (qPCR), chromatin immunoprecipitation (ChIP)-qPCR and electrophoretic mobility shift assays (EMSAs) were conducted to determine the relationship of MYB42 and BRASSINAZOLE-RESISTANT 1 (BZR1), a master switch activating BR signalling.
• **Key Results** MYB42 and MYB85 redundantly and negatively regulate hypocotyl cell elongation. They function in hypocotyl elongation by mediating BR signalling. *MYB42* transcription was suppressed by BR treatment or in *bzr1-1D* (a gain-of-function mutant of BZR1), and mutation of both *MYB42* and *MYB85* enhanced the dwarf phenotype of the BR receptor mutant *bri1-5*. BZR1 directly repressed *MYB42* expression in response to BR. Consistently, hypocotyl length of *bzr1-1D* was increased by simultaneous mutation of *MYB42* and *MYB85*, but was reduced by overexpression of *MYB42*. Expression of a number of BR-regulated BZR1 (non-)targets associated with hypocotyl elongation was suppressed by MYB42, 85. Furthermore, MYB42 enlarged its action in BR signalling through feedback repression of BR accumulation and activation of DOGT1/UGT73C5, a BR-inactivating enzyme.
• **Conclusions** MYB42 inhibits hypocotyl elongation by coordinating BR homeostasis and signalling during primary growth. The present study shows an MYB42, 85-mediated multilevel system that contributes to fine regulation of BR-induced hypocotyl elongation.

Key words: Hypocotyl elongation, MYB transcription factor, BR homeostasis and signalling, feedback regulation, DOGT1/UGT73C5, *Arabidopsis thaliana*.

INTRODUCTION

Brassinosteroids (BRs) are predominant hormones that promote hypocotyl cell elongation. Functional characterization of a subset of Arabidopsis mutants established the BR synthesis and signalling pathways (Kim and Wang, 2010; Oh *et al*., 2014; Nolan *et al*., 2020). The biologically most active BR is brassinolide (BL), which is produced from campesterol in plants. BR signalling through the membrane-localized BR INSENSITIVE1 (BRI1) receptor kinase and intracellular components induces dephosphorylation and accumulation of the central transcription factors BRASSINAZOLE-RESISTANT1 (BZR1) and BRI1-EMS SUPPRESSOR1 (BES1). The activated BZR1 and BES1 promote hypocotyl elongation by mediating regulation of a number of (non-)target genes associated with cell elongation (Sun *et al*., 2010; Yu *et al*., 2011). Also, BZR1 and BES1 directly suppress the expression of BR biosynthetic genes, including *CPD*, *DWF4* and *BR6OX2*, to inhibit BR level. Currently, the mechanism for the integration of BR homeostasis and signalling remains unclear.

R2R3-MYB transcription factors (TFs) are ubiquitously found in plants, and some of its members mediate BR signalling to participate in diverse developmental processes (Dubos *et al*., 2010). In Arabidopsis, MYB30 is directly activated by BES1 and it also cooperates with BES1, coordinately promoting hypocotyl elongation (Li *et al*., 2009). BRASSINOSTEROIDS AT VASCULAR AND ORGANIZING CENTER (BRAVO) is directly suppressed by and physically interacts with BES1, forming a switch that regulates the divisions of the quiescent centre at the root stem cell niche (Vilarrasa-Blasi *et al*., 2014).

WEREWOLF (WER, an MYB protein), GLABRA3 (GL3, a bHLH protein) and TRANSPARENT TESTA GLABRA1 (TTG1, a WD40 protein) form a transcriptional complex that is essential for BR-mediated control of root epidermal cell fate (Cheng *et al*., 2014). Phosphorylation of GL3 and TTG1 by the GSK3-like kinase BIN2 inhibits the activity of this complex. In soybean, overexpression of *GmMYB14* reduces endogenous BR contents, increases high-density yield and improves drought tolerance (Chen *et al*., 2021).

Arabidopsis MYB42 and MYB85 are a pair of paralogous proteins, and they play a redundant role in regulating lignin and phenylpropanoid synthesis during secondary wall formation in stems (Zhong *et al*., 2008; Geng *et al*., 2020). In the present study, we have shown that during the young seedling stage MYB42 inhibits hypocotyl cell elongation by coordinating BR homeostasis and signalling. MYB42 functions as a negative component of the BZR1 pathway. Furthermore, MYB42 can enlarge its action in BR signalling through feedback repression of BR level and activation of DON-GLUCOSYLTRANSFERASE 1 (DOGT1), a BR-inactivating enzyme. Our results suggest that MYB42 might be a node in a transcriptional circuit by which BR regulates cell elongation-associated gene expression.

MATERIALS AND METHODS

Mutant identification and hypocotyl elongation assays

A DNA insertion mutant line for *MYB42* (SALKseq_78190.1) (Geng *et al.*, 2020) was ordered from the Arabidopsis Biological Resource Center. Plants were cultivated in a glasshouse at 23–25 °C and 65 % relative humidity, with a 16-h/8-h light/dark cycle.

For hypocotyl elongation assays, seeds were vernalizated on ½ MS medium at 4 °C and then transferred at 23 °C in darkness for 5 d or under dim light for 7 d. Thirty seedlings were measured using the ImageJ software and an independent experiment was repeated at least three times. The length of epidermal cells was quantified with an Olympus confocal laser scanning microscope (FluoView FV1000). At least 30 seedlings from three independent lines were used for analysis.

GUS staining

A 1.9-kb *MYB42* promoter fragment was fused with β-glucuronidase (GUS) in the DX2181 vector. The resulting construct was transformed into wild-type (WT) plants by *Agrobacterium tumefaciens* (GV3101)-mediated floral-dip method. T_0 transgenic seeds were screened on ½ MS containing 50 mg L^{-1} hygromycin and T_3 homozygous seedlings were used for detection of GUS activity following our previous method (Chai *et al*., 2015).

Construction of recombinant vector and generation of transgenic plants

The coding regions of *MYB42*, *MYB85* and *DOGT1* were individually inserted into the pEARLY100 vector (Invitrogen) to create the overexpression constructs. A 359-bp cDNA fragment of *MYB85* was inserted into pUCCRNAi in an inverted repeat orientation, forming a stem-loop structure. The *MYB85* RNA interference (RNAi) construct was generated by introducing this stem-loop fragment into pCAMBIA 1300. The overexpression and RNAi constructs were transformed into WT or *myb42* plants. The *MYB85 RNAi;myb42* plants were crossed with *bri1-5* (a loss-of-function mutant of BRI1), *bzr1-1D* (a gain-of-function mutant of BZR1) or *DOGT1* overexpression lines (female parent). *MYB42* overexpression plants were introduced into *bzr1-1D* or *MYB85 RNAi;myb42* plants. Homozygous lines from F_2 segregating populations were determined by sequencing, PCR and morphological observation.

Transcription activation assays

Transcription activation assays (TAAs) were carried out in Arabidopsis leaf protoplasts as described previously (Chai *et al*., 2015). A 1782-bp *MYB42* promoter fragment was fused with the *GUS* gene in the modified pBI221 vector to generate the reporter construct. The coding region of *BZR1* was inserted into the modified pBI221 vector to generate the effector construct. In each experiment, the 35S promoter-driven *LUCIFERASE* (*LUC*) reporter gene was used as a control to normalize the data. TAAs were conducted more than three times independently, and an average value was determined.

Electrophoretic mobility shift assays (EMSAs)

EMSAs were conducted as described by Chai *et al*. (2014). The coding region of *BZR1* was fused to the MBP tag in pMAL-c4X and the recombinant protein was purified with amylose resin beads. A biotin-labelled synthetic oligonucleotide covering an E-box site (CAAGTG) in the *MYB42* promoter was used as the probe (BGI, Supplementary Data Table S1). The E-box site is known to be recognized by BZR1 protein (Sun *et al*., 2010). Biotin-labelled DNA was detected by chemiluminescence according to the instructions provided by the manufacturer of the LightShift Chemiluminescent EMSA Kit (Thermo Fisher). EMSAs were performed at least three times independently.

Chromatin immunoprecipitation (ChIP)-qPCR

The ChIP samples were prepared from 10-d-old WT (control) and *mx3* (*pBZR1:mBZR-CFP*) plants following the manufacturer's instruction for the EZ CHIP Kit (Millipore). The amounts of precipitated DNA fragments were detected by quantitative PCR (qPCR) using gene-specific primers (Supplementary Data Table S1). ChIP enrichment was calculated as the ratio between BR-treated and control samples. ChIP-qPCR assays were conducted at least three times independently.

RNA-seq

WT and *MYB85RNAi;myb42* seedlings were grown on ½ MS containing 0 or 0.02 μM propiconazole (PCZ, an alternative

to the BR inhibitor brassinazole) for 5 d in darkness. Total RNAs were isolated from the hypocotyls using TRIzol reagent (Invitrogen). Three biological repeats were set. Each sample includes three independent lines with at least 100 plants. mRNA libraries were sequenced on an Illumina HiSequation 2500 platform (Annoroad Gene Technology). The reads were aligned to the Arabidopsis genome (version TAIR10) using TopHat2 with default parameters (Kim *et al*., 2013). Those genes with fragment per kilobase of exon per million (FPKM) < 1 were excluded from the analysis. Differentially expressed genes (DEGs) were determined based on the criterion of the $|\log_2 \text{fold change}| > 1$ and false discovery rate (FDR) < 0.05.

qRT-PCR

qRT-PCR assay was completed with a SYBR Green Realtime PCR kit (Takara). The reaction was performed with a LightCycler 480 system (Roche) following the method described by Chai *et al*. (2015). *ACTIN2* was used as a reference gene. The relative changes in gene expression were analysed using the $2^{-\Delta\Delta CT}$ method (Livak and Schmittgen, 2001). For each genotype, three biological replicates were used.

Quantification of BR

Approximately 6 g aerial plant parts per repeat were harvested from 4-week-old WT and six *MYB42* overexpression lines grown in soil. The contents of BL and castasterone (CS) were quantified by liquid chromatography tandem mass spectrometry (LC-MS/MS) following a previously reported method (Ding *et al*., 2013) (Wuhan Greensword Creation Technology Company). For each genotype, three biological replicates were set.

RESULTS

MYB42 is highly expressed in the vascular tissues of seedling

To investigate the tissue expression pattern of *MYB42* during primary growth, we detected GUS activity in transgenic plants expressing *proMYB42:GUS* at the seedling stage. Strong GUS staining was visible in the cotyledons, hypocotyls and roots of 7-d-old transgenic seedlings (Fig. 1A). After 14 d of growth, GUS signals were also detected in the vasculature and trichome of true leaves, in addition to the above tissues (Fig. 1B, C). In darkness, strong GUS signals were observed in the elongated hypocotyls, unopened cotyledons and shortened roots of etiolated seedlings (Fig. 1D). These results revealed a potential role of MYB42 in the vascular tissues during the seedling stage.

MYB42 negatively controls hypocotyl elongation

To identify the biological function of MYB42 during primary growth, we generated transgenic lines over-expressing *MYB42* or its paralogue *MYB85*. *MYB85* was used as a control because *MYB42* and *MYB85* redundantly regulate secondary wall formation in Arabidopsis stems (Zhong *et al*., 2008; Geng *et al*., 2020). At least 30 overexpression lines were obtained for each gene (Supplementary Data Fig. S1A, B). All these overexpression lines exhibited shorter hypocotyls and shortened hypocotyl epidermal cells in darkness, relative to WT seedlings (Fig. 2A–C; Fig. S2). This indicated the possible negative roles of *MYB42* and *MYB85* in regulating hypocotyl elongation.

To examine whether *MYB42* is required for hypocotyl elongation, we identified a *MYB42* T-DNA insertion line that was used previously (Geng *et al*., 2020). RT-PCR analysis of *MYB42* transcription indicated that this mutant line is a knockout allele (Supplementary Data Fig. S1C). Statistical analysis of hypocotyl length revealed no apparent difference between dark-grown *myb42* and WT seedlings (Fig. 2A–C). To overcome the functional redundancy of MYB42 and MYB85, we generated RNAi transgenic plants of *MYB85* in an *myb42* background (Fig. S1D). Five-day-old *MYB85RNAi;myb42* seedlings displayed longer hypocotyls and epidermal cells than WT seedlings in darkness (Fig. 2A–C; Fig. S2). This further confirmed the redundant and essential roles of MYB42/85 in controlling hypocotyl elongation. The hypocotyl length of *MYB85RNAi;myb42* plants was restored to the WT-like level by overexpression of *MYB42* (Fig. 2D), indicating that *MYB42* overexpression is sufficient to inhibit hypocotyl elongation.

MYB42 functions as a positive component of the BR pathway

BRs are a group of predominant hormones promoting plant cell elongation (Nolan *et al*., 2020). To examine the association of MYB42-mediated inhibition of cell elongation with BR response, we first investigated whether 2,4-epibrassinolide (2,4-eBL) treatment affects *MYB42* (*MYB85* as control) transcription. The expression level of *MYB42* in WT plants was rapidly decreased to 5 % of basal level at 1 h, and remained stable until 72 h (Supplementary Data Fig. S3A). A similar expression pattern was observed for *MYB85* in response to BL treatment. We further detected the responses of WT, *MYB42OE* and *MYB85RNAi;myb42* seedlings to PCZ, a BR biosynthesis inhibitor. With PCZ treatment, hypocotyl elongation of the three genotypes was inhibited to varying degrees (Fig. 3A, B). The strongest inhibition was observed in *MYB85RNAi;myb42* plants (51.9 %), followed by WT plants (42.3 %) and the weakest inhibition in *MYB42OE* plants (37.5 %). All these results indicated that MYB42 may inhibit hypocotyl elongation by mediating BR signalling.

To determine the genetic interaction between MYB42 and the receptor BRI1 of BRs, we crossed *MYB85RNAi;myb42* plants with the *bri1-5* mutant that shows a semi-dwarf phenotype (Noguchi *et al*., 1999). Mutation of both *MYB42* and *MYB85* slightly enhanced the phenotype of *bri1-5* on ½ MS or in soil (Fig. 3C, D; Supplementary Data Fig. S3B). *MYB85RNAi;myb42/bri1-5* plants exhibited downward-curling cotyledons, shorter inflorescence stems and smaller leaves compared with *bri1-5* under light, and they displayed visibly shorter hypocotyls in darkness. These results, combined with the PCZ responses of *MYB42OE* and *MYB85RNAi;myb42* plants (Fig. 3B), indicated that MYB42 may function as a positive component of the BR pathway.

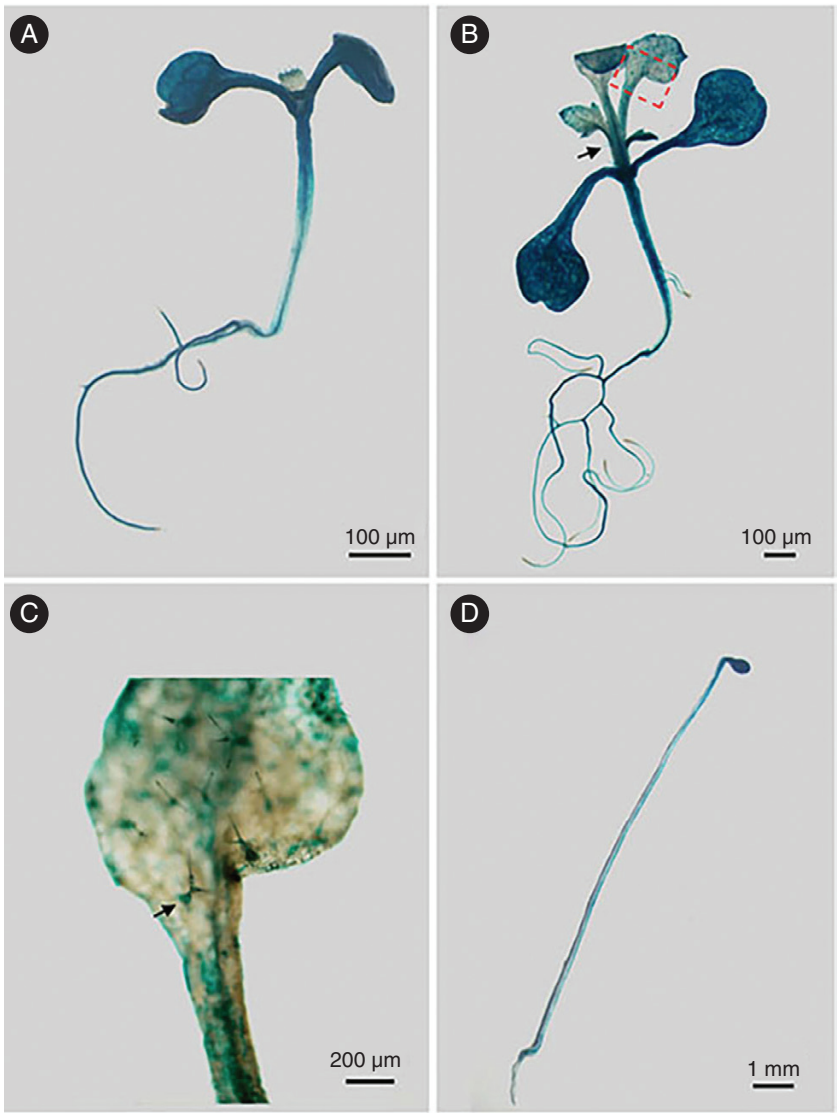

Fig. 1. Histochemical analysis of *MYB42* expression during the seedling stage. (A–D) The expression patterns of *MYB42* in 7-d-old (A) or 14-d-old (B and C) *proMYB42-GUS* plants under light, or in 5-d-old plants in darkness (D), detected by *GUS* reporter gene. The partial leaf region (red box) is enlarged in C. A stained trichome is shown by a black arrow.

BR promotes BZR1 targeted MYB42 to control hypocotyl elongation

BZR1 promotes hypocotyl elongation by activating or suppressing the expression of a huge number of cell elongation-associated genes (Oh *et al*., 2014). To examine the relationship of BZR1 and MYB42, we first detected *MYB42* transcription in WT (control) and *bzr1-1D* plants in the absence or presence of BR. The *MYB42* expression level was 79 % lower in *bzr1-1D* than that in WT plants (Fig. 4A). When treated with 2,4-eBL, *MYB42* expression was inhibited by 50 % in WT plants, but was not significantly altered in *bzr1-1D*. This was consistent with a previous description that *bzr1-1D* is insensitive to BRZ treatment in darkness (Wang *et al*., 2002). To validate the suppression of *MYB42* expression by BZR1, transient expression assays were conducted in Arabidopsis leaf mesophyll protoplasts. Lower GUS activity was observed in the protoplasts transfected with *35S:BZR1* and *MYB42pro:GUS* than that in the protoplasts with *35S:BZR1* and empty vector (Fig. 4B, C). All these results indicated that BZR1 may repress *MYB42* expression in BR signalling.

Analysis of the 2000-bp *MYB42* promoter sequence showed an E-box site (CAAGTG) that is recognized by BZR1 (Sun *et al*., 2010), 1478 bp upstream of the translation initiation site. This promoted us to investigate whether BZR1 could recognize this E-box site in the *MYB42* promoter. EMSA data revealed that MBP-BZR1 protein bound to a fragment from the *MYB42* promoter that contained the E-box (Fig. 4D). Addition of the unlabelled promoter fragment efficiently competed with labelled probe, indicating a specific binding of BZR1 to this fragment *in vitro*. Using ChIP-qPCR assays, we demonstrated that BZR1 was significantly enriched at the E-box (−1478 bp) but not at control (−274 bp) in the promoter of *MYB42* in *mx3* (*pBZR1:mBZR1-CFP*) seedlings (Fig. 4E). BR treatment further enhanced the binding of BZR1 to this E-box site in the *MYB42* promoter (Fig. 4E). These results indicated that *MYB42* may be a negative target of BZR1 in BR signalling.

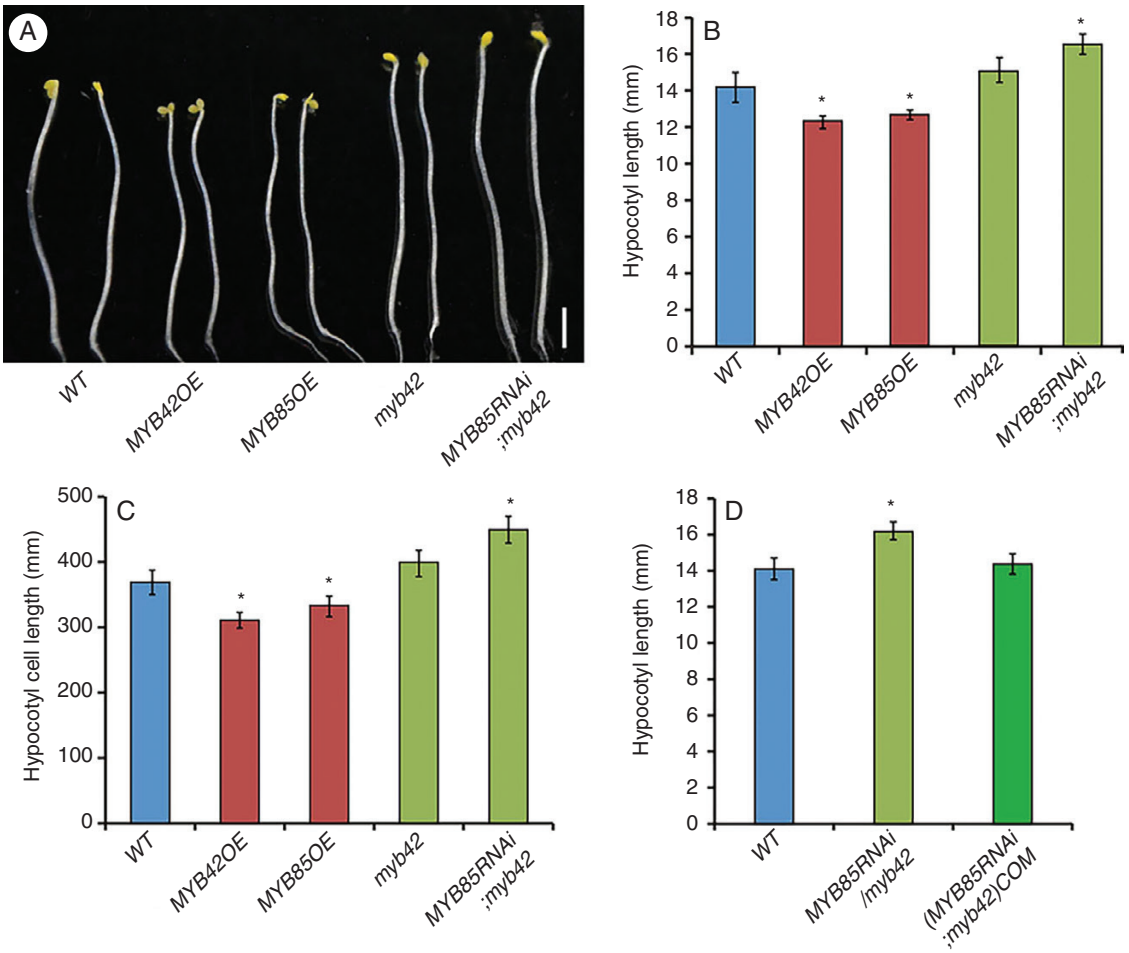

FIG. 2. MYB42 and its paralogue MYB85 redundantly inhibit hypocotyl cell elongation. (A–C) Hypocotyls of 5-d-old dark-grown wild-type (WT), *MYB42/MYB85* overexpression, *myb42* and *MYB85 RNAi;myb42* plants. Similar phenotypes were observed among different lines of each genotype, and a representative line is shown. Bar = 50 µm. (D) Hypocotyl length of *MYB85RNAi;myb42* plants was restored to the WT-like level by *MYB42* overexpression. Statistical analysis was conducted from more than three lines for each transgenic genotype. Data are the means ± s.d. of 30–40 plants in each line. Student's *t*-test, $*P < 0.05$.

To determine whether BZR1-targeted MYB42 affects hypocotyl elongation in response to BR, we generated *MYB42OE/bzr1-1D* and *MYB85 RNAi;myb42/bzr1-1D* plants. No apparent difference in hypocotyl length was observed between *bzr1-1D* and the WT in darkness (Fig. 4F, left), which is consistent with the description by Wang *et al*. (2002). However, the hypocotyl length of *bzr1-1D* was reduced by overexpression of *MYB42*, and was increased by simultaneous mutation of *MYB42* and *MYB85* (Fig. 4F, left). The insensitivity of *bzr1-1D* to PCZ treatment was also weakened in the *MYB85 RNAi;myb42* background (Fig. 4F, right). These results indicated that BZR1 promotes hypocotyl elongation probably by MYB42 and MYB85 in the BR pathway.

A number of BR-regulated BZR1 (non-)targets show altered expression levels in MYB85RNAi/myb42 plants with PCZ treatment

To explore the MYB42-mediated regulatory network in BR signalling, we performed RNA-sequencing (RNA-seq) analysis with 5-d-old dark-grown WT and *MYB85RNAi;myb42* plants in the absence or presence of PCZ. Using the stringent criteria $|\log_2 FC| > 1$ and FDR < 0.05, we obtained 1943 PCZ-responsive genes in WT plants and 1273 PCZ-responsive genes in *MYB85RNAi;myb42* plants (Supplementary Data Table S2). A total of 1401 genes were defined as PCZ-responsive, MYB42/85-dependent genes based on the classification as follows: Group I, 1275 PCZ-responsive genes that were upregulated or downregulated in WT plants but not in *MYB85RNAi;myb42* plants; and Group II, 126 genes with at least 1.5-fold higher or lower expression in *MYB85RNAi;myb42* plants than in WT plants with PCZ treatment (Table S3).

Genes regulated by BR and BRZ (a BR biosynthetic inhibitor) show a strong inverse correlation (Li *et al*., 2009). To investigate how MYB42 mediates BZR1 signalling to regulate hypocotyl elongation, we compared 1401 PCZ-responsive, MYB42/85-dependent genes with 953 BR-regulated BZR1 targets or 1789 BZR1-regulated non-targets (Sun *et al*., 2010; Oh *et al*., 2012). In total, 8.8 % (84/953) of BZR1 targets and 9.4 % (168/1789) of BZR1-regulated non-targets were affected by MYB42/85 in BR signalling in darkness (Fig. 5A; Supplementary Data Table S4). Of these, we further analysed two BR-regulated BZR1 targets [*EXPANSIN A1* (*EXPA1*) and

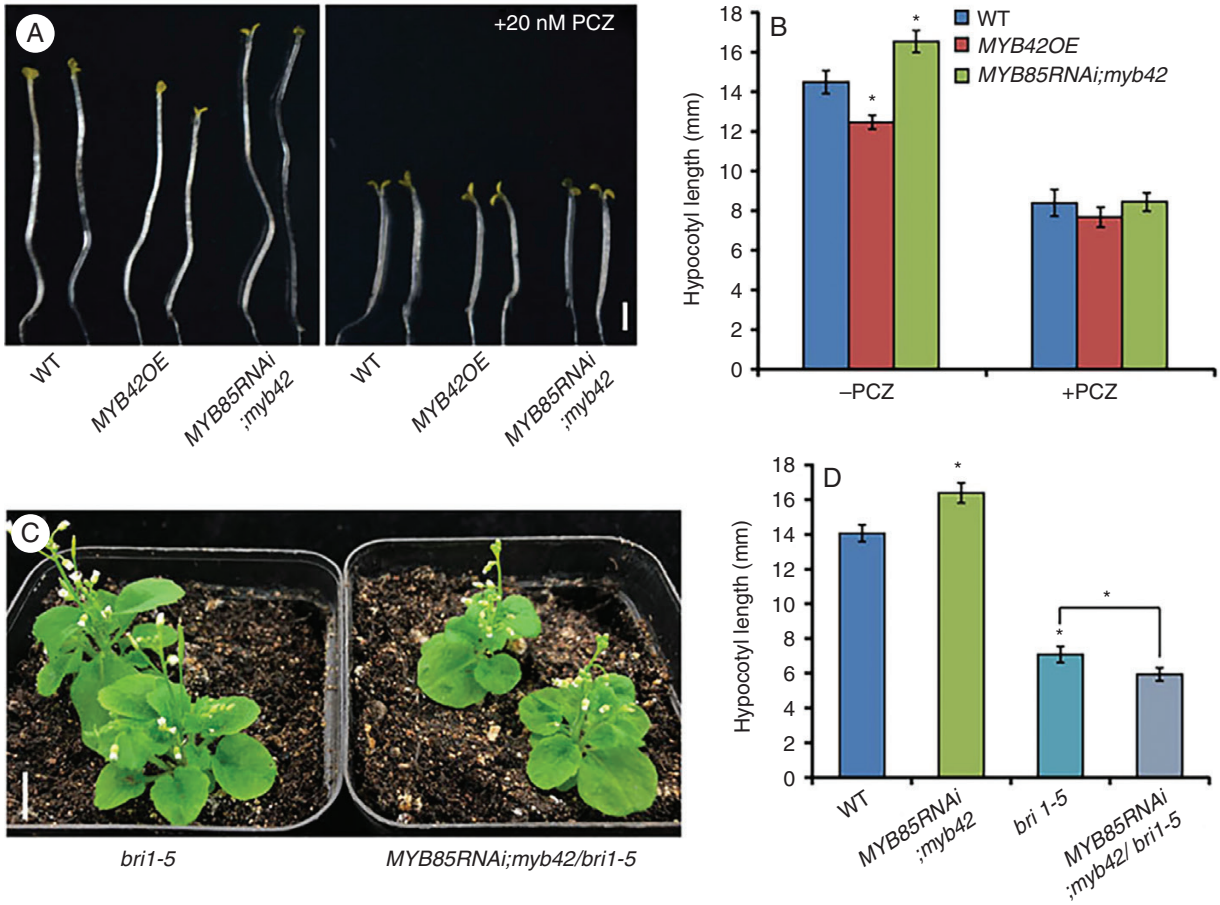

Fig. 3. MYB42 is a positive component of the BR pathway. (A, B) Hypocotyls of 5-d-old WT, *MYB42OE* and *MYB85RNAi;myb42* plants in darkness in the presence or absence of 0.02 μM propiconazole (PCZ, a BR biosynthesis inhibitor). (C) Five-week-old *bri1-5* (a BRI1 mutant allele) and *MYB85RNAi;myb42/bri1-5* plants in soil. (D) Hypocotyl length measurement of 5-d-old WT, *MYB85RNAi;myb42*, *bri1-5* and *MYB85RNAi;myb42/bri1-5* plants. Statistical analysis was conducted from more than three lines for each transgenic genotype. Data are the means ± s.d. of 30 plants in each line. *t*-test, $*P < 0.05$. Bar = 1 mm in A and 1 cm in C.

GA20OX1], two BZR1-regulated non-targets [*EXPA5* and *XYLOGLUCAN ENDOTRANSGLUCOSYLASE/HYDROLASE 19* (*XTH19*)] and two MYB42/85-regulated specific genes [*1-AMINOCYCLOPROPANE-1-CARBOXYLATE SYNTHASE* (*ACS8*) and *PIN-FORMED 5* (*PIN5*)] (Fig. 5B). *EXPA5* and *XTH19* participate in BR-induced hypocotyl elongation, and *EXPA1* is essential for hypocotyl elongation (Park *et al.*, 2010; Miedes *et al.*, 2013; Ilias *et al.*, 2017; Xu *et al.*, 2020). *PIN5* is an auxin efflux carrier, and *GA20OX1* and *ACS8* are responsive for the biosynthesis of gibberellin (GA) and ethylene, respectively. Auxin, GA and ethylene are known to interact with BRs to regulate hypocotyl cell elongation (Peres *et al.*, 2019). In our RNA-seq data, the expression levels of *EXPA1*, *EXPA5*, *XTH19*, *GA20OX1* and *ACS8* were markedly reduced and *PIN5* expression level was increased in WT plants when treated with PCZ (Fig. 5B). This is consistent with a previous description that expression levels of *EXPA1*, *EXPA5*, *XTH19* or *GA20OX1* are higher in *bzr1-1D* than in WT plants (Oh *et al.*, 2012). Moreover, in the *MYB85RNAi;myb42* background, PCZ-repressed expression of *EXPA1*, *EXPA5*, *XTH19*, *GA20OX1* and *ACS8* and PCZ-activated expression of *PIN5* were largely attenuated, as was further confirmed by qRT-PCR assays (Fig. 5B, C). Collectively, these results indicated that MYB42 and BZR1 coordinately control hypocotyl elongation probably by regulating expression of a number of common genes.

To determine how MYB42 affects BZR1-mediated regulation of hypocotyl elongation, we detected the expression levels of *EXPA1* and *EXPA5*, two BZR1-induced genes, in PCZ-treated or untreated WT, *MYB85RNAi;myb42*, *bzr1-1D* and *MYB85RNAi;myb42/bzr1-1D* plants. As shown in Fig. 5D, expression levels of *EXPA1* and *EXPA5* were higher in *bzr1-1D* or *MYB85RNAi;myb42* plants than in WT plants, and such expression in *MYB85RNAi;myb42* plants was enhanced by introduction into *bzr1-1D*. With PCZ treatment, expression levels of *EXPA1* and *EXPA5* were reduced by 50 % in WT plants, but showed slight reductions in *bzr1-1D*, *MYB85RNAi;myb42* and *MYB85RNAi;myb42/bzr1-1D* plants. These results suggested that MYB42 inhibits hypocotyl elongation possibly by partially inhibiting BZR signalling.

MYB42 involves feedback regulation of BR homeostasis

PCZ-responsive, MYB42/85-dependent genes contained *DOGT1/UGT73C5* (Supplementary Data Table S2), which encodes an enzyme glucosylating BRs and reducing the

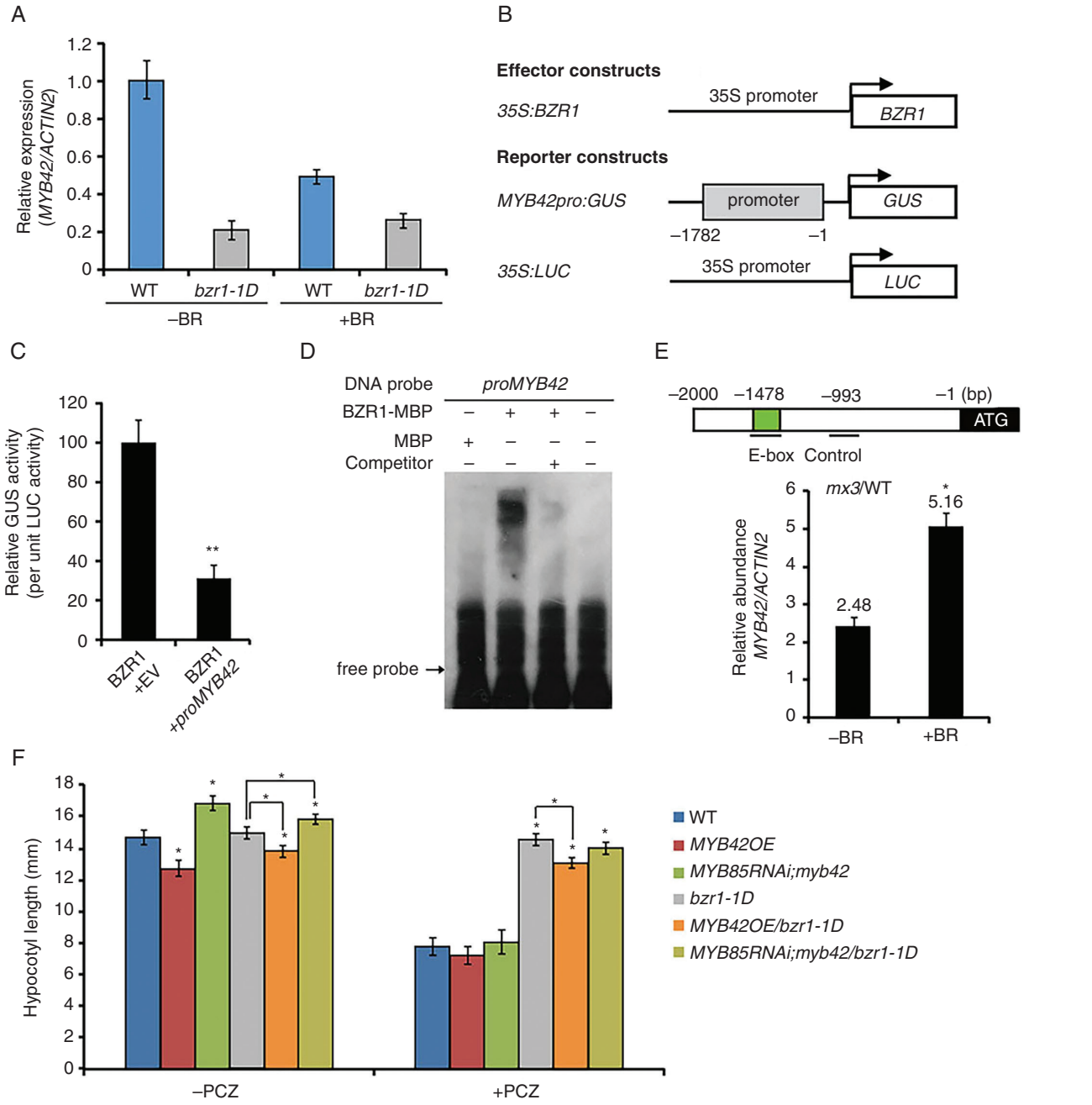

FIG. 4. *MYB42* expression is directly repressed by BRZ1 in BR signalling. (A) qRT-PCR showing *MYB42* expression in 10-d-old WT and *bzr1-1D* plants in the absence or presence of 1 μM 24-eBL. (B, C) Transcription activity assays showing that BZR1 represses the *MYB42* promoter-driven *GUS* expression in Arabidopsis leaf protoplasts. GUS activity in the protoplasts co-transformed with BZR1 and empty vector (EV) was set to 1. The expression of *LUC* was used as a control for normalization. Data are means ± s.d. of three independent experiments. (D) EMSA showing the specific binding of BZR1 to an E-box site (CAAGTG) in the *MYB42* promoter *in vitro*. (E) ChIP-qPCR on 10-d-old WT and *pBZR1:mBZR1-CFP* (*mx3*) plants with or without 24-eBL showing that BR induction increased the binding of BZR1 to the E-box site in the *MYB42* promoter *in vivo*. A non-binding site of BZR1 in the *MYB42* promoter was used as a control for normalization. Data are the means ± s.d. of triplicate experiments. (F) Hypocotyl length measurement of 5-d-old dark-grown WT, *MYB42OE*, *MYB85RNAi;myb42*, *bzr1-1D*, *MYB42OE/bzr1-1D* and *MYB85RNAi;myb42/bzr1-1D* plants with or without PCZ treatment. Statistical analysis was conducted from more than three lines for each transgenic genotype. Data are the means ± s.d. of 30 seedlings in each line. *t*-test, $*P < 0.05$.

activity of BRs (Poppenberger *et al.*, 2005). This promoted us to investigate whether MYB42 involves feedback regulation of BR activity during hypocotyl growth. Compared with WT plants, the expression level of *DOGT1* was reduced in *MYB85 RNAi;myb42* plants but increased in *MYB42OE* plants (Fig. 6A). This indicated that MYB42 may up-regulate *DOGT1* expression. To test the association of MYB42-inhibited hypocotyl elongation with DOGT1, we generated transgenic plants over-expressing *DOGT1* (*DOGT1OE*) and then introduced the representative overexpression lines into *MYB85 RNAi;myb42* plants. The *DOGT1OE* plants, like BR-deficient mutants, showed shortened stems and

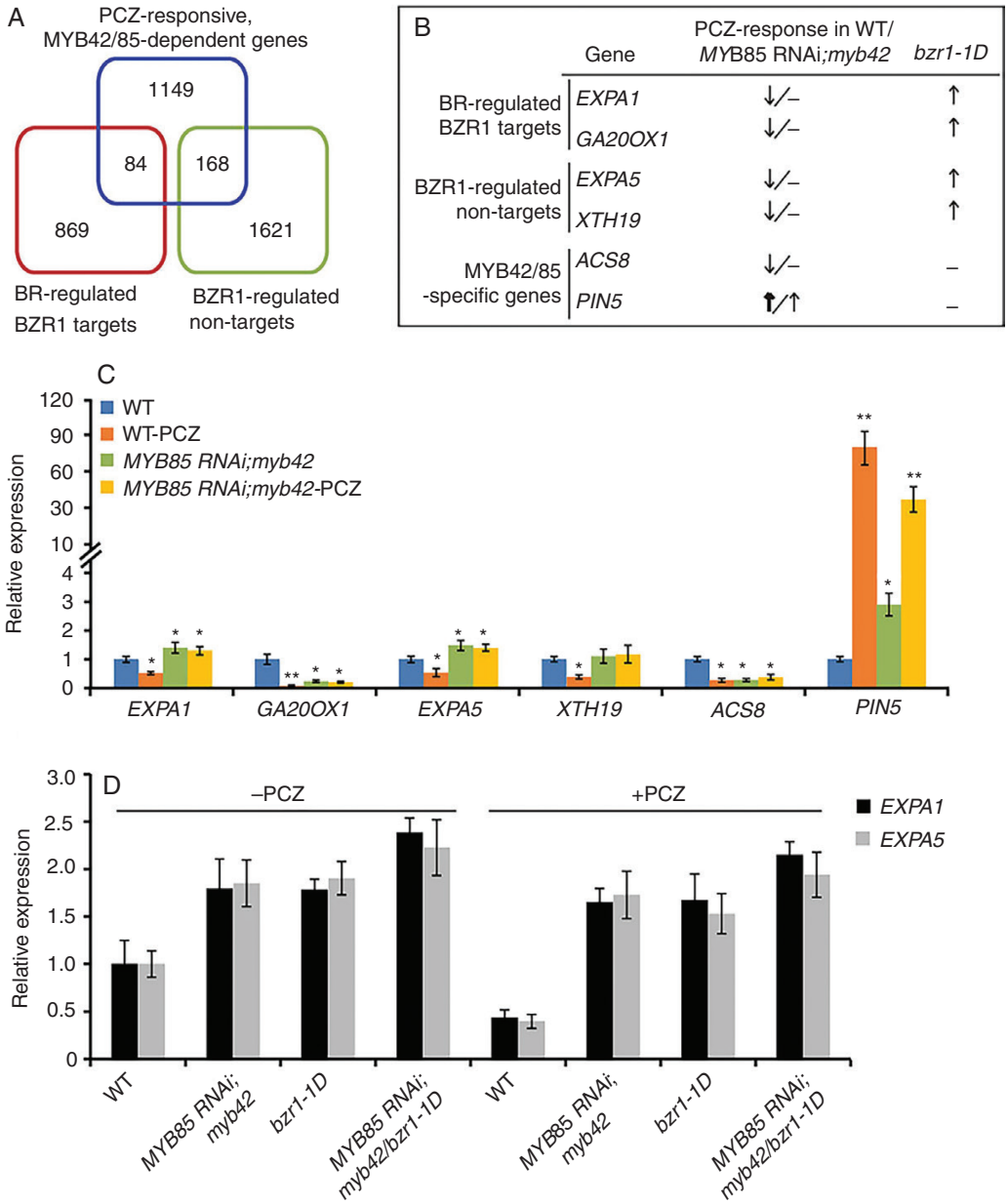

FIG. 5. MYB42 influences BZR1 regulation of cell elongation-associated targets and non-targets. (A) Venn diagram of PCZ-responsive MYB42/85-dependent genes and BR-regulated BZR1 targets or BZR1-regulated non-targets. PCZ-responsive MYB42/85-dependent genes are shown in Supplementary Data Table S3. (B) Partial cell elongation-associated genes from A. (C) Expression of six genes (B) in 5-d-old WT and *MYB85RNAi;myb42* plants in darkness with or without PCZ treatment. *t*-test, $*P < 0.05$; $**P < 0.01$. (D) Expression of *EXPA1* and *EXPA5* in 5-d-old WT, *MYB85RNAi;myb42*, *bzr1-1D* and *MYB85RNAi;myb42/bzr1-1D* plants in darkness with or without PCZ treatment. For qRT-PCR, data are expressed as the means ± s.d. from three biological replicates.

hypocotyls, small leaves, and partial fertility (Fig. 6B, C; Fig. S4). These growth defects of *DOGT1* overexpression plants were also described previously (Poppenberger *et al.*, 2005). Statistical analysis of hypocotyl length in *DOGT1OE* seedlings was performed on experiments under dim light, because overexpression of *DOGT1* inhibits hypocotyl elongation under light, but not in darkness (Poppenberger *et al.*, 2005). The results revealed that mutation of both *MYB42* and *MYB85* in *DOGT1OE* plants resulted in an apparent increase in both sterility and length of stems and hypocotyls (Fig. 6B, C; Fig. S4). These results indicated that MYB42/85 inhibits hypocotyl elongation possibly by activation of the BR-inactivating enzyme DOGT1.

We further investigated whether overexpression of *MYB42* affects endogenous BR levels. BR contents were detected in aerial plant parts of six *MYB42OE* lines (WT as a control) by LC-MS/MS according to the method described previously (Poppenberger *et al.*, 2005; Husar *et al.*, 2011). As shown in Fig. 6D, the level of CS (the direct precursor of BL) was reduced in *MYB42OE* plants in comparison to WT plants. BL was below the limit of detection in both genotypes, similar to a previous description (Husar *et al.*, 2011). Together, these data

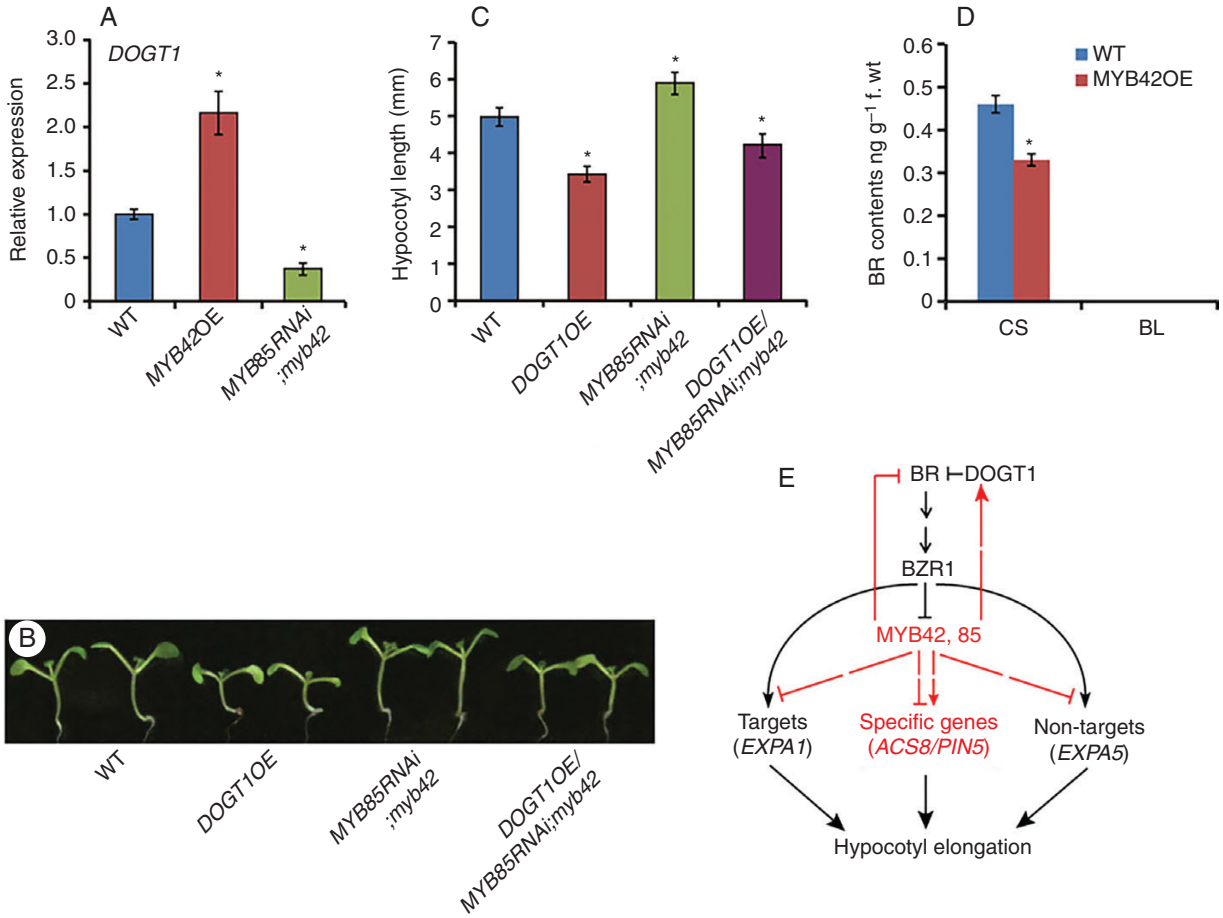

FIG. 6. MYB42 involves feedback regulation of BR homeostasis. (A) qRT-PCR showing *DOGT1* expression levels in 10-d-old WT, *MYB42OE* and *MYB85RNAi;myb42* plants. (B, C) Hypocotyl length of 7-d-old WT, *DOGT1OE*, *MYB85 RNAi;myb42* and *DOGT1OE/MYB85RNAi;myb42* plants under dim light. Statistical analysis was conducted from more than three lines for each transgenic genotype. Data are the means ± s.d. of 30 plants in each line. (D) Levels of BRs (CS, castasterone; BL, brassinolide) in WT and *MYB42OE* plants detected by LC-MS/MS analysis; f.wt, fresh weight. BL was not detected in either genotype. (E) A model of MYB42 and MYB85 function in BR-induced cell elongation. MYB42, 85 may enlarge their action in BR signalling and cell elongation by a feedback loop. The pathway identified in this study is shown with red. In A, C and D, *t* test, $*P < 0.05$.

indicated that MYB42 may inhibit BR homeostasis by a feedback loop.

DISCUSSION

MYB42 and MYB85 play dual roles in primary and secondary cell wall formation

Primary cell walls (capable of expanding in area) and secondary cell walls (incapable of expanding) have different cellular locations and polysaccharide compositions (Srivastava *et al.*, 2017). Primary cell walls are more easily deconstructed due to their flexible features, while secondary cell walls are largely recalcitrant to microbial degradation. Generally, the formation of primary and secondary walls is regulated by different systems. Several recent studies in Arabidopsis have shown the dual roles of TFs in regulating the two types of cell walls. Transgenic plants overexpressing the group IIId and IIIe AP2/ERF TFs in mutants lacking secondary walls show thickened cell wall characteristics of primary cell walls (Sakamoto *et al.*, 2018). The homeodomain TF KNAT7 mediates the regulation of primary and secondary wall formation in seeds and stems, respectively (Li *et al.*, 2011; Qin *et al.*, 2020; Wang *et al.*, 2020*a*, *b*).

In this study, we identified MYB42 and MYB85 as another regulator of primary and secondary wall formation. During mature stages, MYB42 and MYB85 are down-regulated by SECONDARY WALL-ASSOCIATED NAC DOMAIN PROTEIN1 (SND1), a first-layer master switch activating secondary wall biosynthesis in Arabidopsis stems (Zhong *et al.*, 2008). The dominant repressor of *MYB85* has thinner fibre cell walls, while overexpression of *MYB85* causes ectopic accumulation of lignin in cortical and epidermal cells (Zhong *et al.*, 2008). Furthermore, MYB42, 85 and other two homologues MYB20, 43 redundantly regulate lignin biosynthesis and they also directly activate the expression of *MYB4*, specifically inhibiting flavonoid biosynthesis (Geng *et al.*, 2020).

During seedling stages, MYB42 and MYB85 redundantly inhibit hypocotyl elongation. The *myb42* single mutant exhibited a similar phenotype to WT plants, but a reduced level of *MYB85* in *myb42* resulted in a significant increase in hypocotyl length compared with WT plants. *MYB42* overexpression was sufficient to inhibit hypocotyl cell elongation in WT plants and

to restore the hypocotyl length of *MYB85 RNAi;myb42* to the WT level. Therefore, MYB42 and MYB85, like KNAT7, may regulate hypocotyl elongation and secondary wall biosynthesis in different pathways at different developmental stages.

MYB42 inhibits hypocotyl elongation by coordinating BR homeostasis and signalling

BRs are steroidal phytohormones that are essential for hypocotyl cell elongation (Oh *et al*., 2014; Nolan *et al*., 2020). Currently, it remains unclear about the transcriptional regulation of BR homeostasis and signalling. Here, we have demonstrated that MYB42 is capable of partially inhibiting BZR1 signalling and promoting BR inactivation. Genetic and biochemical data revealed that MYB42 was a negative target of BZR1 and acted as a positive component of the BR pathway. Consistently, the hypocotyl length of *bzr1-1D* was increased in *MYB85 RNAi;myb42* plants, but reduced in *MYB42* overexpression plants in terms of genetics. Comparison of transcriptome data showed that 18.2 % of BZR1-regulated genes were affected by MYB42/85 in BR signalling, of which some cell elongation-associated genes were down-regulated by MYB42, implying a partial inhibition of BZR1-induced hypocotyl elongation by MYB42.

In contrast to our understanding of feedback repression of BR biosynthetic genes by BZR1, the mechanisms underlying BR inactivation are largely unclear. It is known that DOGT1/UGT73C5 mediates the glucosylation of BL and CS at the 23-OH position and causes BR-deficient phenotypes (Poppenberger *et al*., 2005). Our current results revealed that MYB42 activated *DOGT1* expression and mutation of both *MYB42* and *MYB85* attenuated DOGT1-mediated inhibition of hypocotyl elongation. Furthermore, the CS level was reduced in *MYB42* overexpression lines compared with WT plants. Thus, it is possible that MYB42, 85 enlarge their action in BR signalling through feedback activation of *DOGT1* expression and repression of BR accumulation. Based on our observations, we propose that MYB42 and MYB85 might function in hypocotyl elongation by coordinating BR homeostasis and signalling (Fig. 6D). These results provide novel insight into the gene network of BR-induced hypocotyl elongation.

SUPPLEMENTARY DATA

Supplementary data are available online at https://academic.oup.com/aob and consist of the following. Fig. S1: Identification of *MYB42* or *MYB85* overexpression, *myb42*, and *MYB85 RNAi;myb42* plants. Fig. S2: Hypocotyl epidermal cells of 5-d-old dark-grown WT, *MYB42* or *MYB85* overexpression, and *MYB85RNAi;myb42* plants. Fig. S3: MYB42 and MYB85 are associated with BR signalling. Fig. S4: Phenotypes of 8-week-old WT, *DOGT1OE* and *DOGT1OE/MYB85RNAi;myb42* plants. Table S1: Primers used in this study. Table S2: Differentially expressed genes in wild-type or *MYB85RNAi/myb42* plants in response to PCZ. Table S3: 1401 PCZ-responsive MYB42/85-dependent genes. Table S4: Overlap between PCZ-responsive MYB42/85-dependent genes and BR-regulated BZR1 targets.

ACKNOWLEDGMENTS

We thank Professor Ming-yi Bai (Shandong University, China) for providing the *bri1-5, bzr1-1D* and *mx3* seeds.

FUNDING

Financial support was obtained from the National Natural Science Foundation of China (31770315, 31972955, 31972860 and 32101549), Taishan Scholar Program of Shandong (tsqn202103092) and 'First Class Grassland Science Discipline' Program of Shandong Province.

CONFLICT OF INTEREST

The authors declare that they have no no competing interests.

LITERATURE CITED

Chai G, Qi G, Cao Y, *et al.* 2014. Poplar PdC3H17 and PdC3H18 are direct targets of PdMYB3 and PdMYB21, and positively regulate secondary wall formation in Arabidopsis and poplar. *The New Phytologist* **203**: 520–534.

Chai G, Kong Y, Zhu M, *et al.* 2015. Arabidopsis C3H14 and C3H15 have overlapping roles in the regulation of secondary wall thickening and anther development. *Journal of Experimental Botany* **66**: 2595–2609.

Chen L, Yang H, Fang Y, *et al.* 2021. Overexpression of GmMYB14 improves high-density yield and drought tolerance of soybean through regulating plant architecture mediated by the brassinosteroid pathway. *Plant Biotechnology Journal* **19**: 702–716.

Cheng Y, Zhu W, Chen Y, Ito S, Asami T, Wang X. 2014. Brassinosteroids control root epidermal cell fate via direct regulation of a MYB-bHLH-WD40 complex by GSK3-like kinases. *Elife* **3**: e02525.

Ding J, Mao LJ, Wang ST, Yuan BF, Feng YQ. 2013. Determination of endogenous brassinosteroids in plant tissues using solid-phase extraction with double layered cartridge followed by high-performance liquid chromatography-tandem mass spectrometry. *Phytochemical Analysis: PCA* **24**: 386–394.

Dubos C, Stracke R, Grotewold E, Weisshaar B, Martin C, Lepiniec L. 2010. MYB transcription factors in Arabidopsis. *Trends in Plant Science* **15**: 573–581.

Geng P, Zhang S, Liu J, *et al.* 2020. MYB20, MYB42, MYB43, and MYB85 regulate phenylalanine and lignin biosynthesis during secondary cell wall formation. *Plant Physiology* **182**: 1272–1283.

Husar S, Berthiller F, Fujioka S, *et al.* 2011. Overexpression of the UGT73C6 alters brassinosteroid glucoside formation in *Arabidopsis thaliana*. *BMC Plant Biology* **11**: 51.

Ilias IA, Airianah OB, Baharum SN, Goh HH. 2017. Transcriptomic data of *Arabidopsis thaliana* hypocotyl upon suppression of expansin genes. *Genomics Data* **12**: 132–133.

Kim TW, Wang ZY. 2010. Brassinosteroid signal transduction from receptor kinases to transcription factors. *Annual Review of Plant Biology* **61**: 681–704.

Kim D, Pertea G, Trapnell C, Pimentel H, Kelley R, Salzberg SL. 2013. TopHat2: accurate alignment of transcriptomes in the presence of insertions, deletions and gene fusions. *Genome Biology* **14**: R36.

Li E, Wang S, Liu Y, Chen JG, Douglas CJ. 2011. OVATE FAMILY PROTEIN4 (OFP4) interaction with KNAT7 regulates secondary cell wall formation in *Arabidopsis thaliana*. *The Plant Journal: for Cell and Molecular Biology* **67**: 328–341.

Li L, Yu X, Thompson A, *et al.* 2009. Arabidopsis MYB30 is a direct target of BES1 and cooperates with BES1 to regulate brassinosteroid-induced gene expression. *The Plant Journal: for Cell and Molecular Biology* **58**: 275–286.

Miedes E, Suslov D, Vandenbussche F, *et al.* 2013. Xyloglucan endotransglucosylase/hydrolase (XTH) overexpression affects growth and cell wall mechanics in etiolated Arabidopsis hypocotyls. *Journal of Experimental Botany* **64**: 2481–2497.

Nolan TM, Vukašinović N, Liu D, Russinova E, Yin Y. 2020. Brassinosteroids: multidimensional regulators of plant growth, development, and stress responses. *The Plant Cell* **32**: 295–318.

Noguchi T, Fujioka S, Choe S, *et al.* 1999. Brassinosteroid-insensitive dwarf mutants of Arabidopsis accumulate brassinosteroids. *Plant Physiology* **121**: 743–752.

Oh E, Zhu JY, Wang ZY. 2012. Interaction between BZR1 and PIF4 integrates brassinosteroid and environmental responses. *Nature Cell Biology* **14**: 802–809.

Oh E, Zhu J, Bai M, Arenhart RA, Sun Y, Wang Z. 2014. Cell elongation is regulated through a central circuit of interacting transcription factors in the Arabidopsis hypocotyl. *eLife* **3**: e03031.

Park CH, Kim TW, Son SH, *et al.* 2010. Brassinosteroids control AtEXPA5 gene expression in *Arabidopsis thaliana*. *Phytochemistry* **71**: 380–387.

Peres A, Soares JS, Tavares RG, *et al.* 2019. Brassinosteroids, the sixth class of phytohormones: a molecular view from the discovery to hormonal interactions in plant development and stress adaptation. *International Journal of Molecular Sciences* **20**: 331.

Livak KJ, Schmittgen TD. 2001. Analysis of relative gene expression data using real-time quantitative PCR and the 2(-Delta Delta C(T)) method. *Methods (San Diego, Calif.)* **25**: 402–408.

Poppenberger B, Fujioka S, Soeno K, *et al.* 2005. The UGT73C5 of *Arabidopsis thaliana* glucosylates brassinosteroids. *Proceedings of the National Academy of Sciences of the United States of America* **102**: 15253–15258.

Qin W, Yin Q, Chen J, *et al.* 2020. The class II KNOX transcription factors KNAT3 and KNAT7 synergistically regulate monolignol biosynthesis in Arabidopsis. *Journal of Experimental Botany* **71**: 5469–5483.

Sakamoto S, Somssich M, Nakata MT, *et al.* 2018. Complete substitution of a secondary cell wall with a primary cell wall in Arabidopsis. *Nature Plants* **4**: 777–783.

Srivastava V, McKee LS, Bulone V. 2017. *Plant cell walls.* Chichester: eLS. Wiley.

Sun Y, Fan XY, Cao DM, *et al.* 2010. Integration of brassinosteroid signal transduction with the transcription network for plant growth regulation in Arabidopsis. *Developmental Cell* **19**: 765–777.

Vilarrasa-Blasi J, González-García MP, Frigola D, *et al.* 2014. Regulation of plant stem cell quiescence by a brassinosteroid signaling module. *Developmental Cell* **30**: 36–47.

Wang S, Yamaguchi M, Grienenberger E, Martone PT, Samuels AL, Mansfield SD. 2020. The Class II KNOX genes KNAT3 and KNAT7 work cooperatively to influence deposition of secondary cell walls that provide mechanical support to Arabidopsis stems. *The Plant Journal: for Cell and Molecular Biology* **101**: 293–309.

Wang Y, Xu Y, Pei S, *et al.* 2020. KNAT7 regulates xylan biosynthesis in Arabidopsis seed-coat mucilage. *Journal of Experimental Botany* **71**: 4125–4139.

Wang ZY, Nakano T, Gendron J, *et al.* 2002. Nuclear-localized BZR1 mediates brassinosteroid-induced growth and feedback suppression of brassinosteroid biosynthesis. *Developmental Cell* **2**: 505–513.

Xu P, Fang S, Chen H, Cai W. 2020. The brassinosteroid-responsive xyloglucan endotransglucosylase/hydrolase 19 (XTH19) and XTH23 genes are involved in lateral root development under salt stress in Arabidopsis. *The Plant Journal: for Cell and Molecular Biology* **104**: 59–75.

Yu X, Li L, Zola J, *et al.* 2011. A brassinosteroid transcriptional network revealed by genome-wide identification of BESI target genes in *Arabidopsis thaliana*. *The Plant Journal: for Cell and Molecular Biology* **65**: 634–646.

Zhong R, Lee C, Zhou J, McCarthy RL, Ye ZH. 2008. A battery of transcription factors involved in the regulation of secondary cell wall biosynthesis in Arabidopsis. *The Plant Cell* **20**: 2763–2782.